

## REVIEW ARTICLE

# The effects of plateau subduction on plate bending, stress and intraplate seismicity

Jiangyang Zhang<sup>1,2</sup> | Fan Zhang<sup>2,3,4</sup> | Hongfeng Yang<sup>5,1</sup> | Jian Lin<sup>2,4,6,7</sup> | Zhen Sun<sup>2,3,4</sup>

<sup>1</sup>Shenzhen Research Institute, The Chinese University of Hong Kong, Shenzhen, China

<sup>2</sup>Key Laboratory of Ocean and Marginal Sea Geology, South China Sea Institute of Oceanology, Innovation Academy of South China Sea Ecology and Environmental Engineering, Chinese Academy of Sciences, Guangzhou, China

<sup>3</sup>Southern Marine Science and Engineering Guangdong Laboratory (Guangzhou), Guangzhou, China

<sup>4</sup>China-Pakistan Joint Research Center on Earth Sciences, CAS-HEC, Islamabad, Pakistan

<sup>5</sup>Earth System Science Program, Chinese University of Hong Kong, Hong Kong, China

<sup>6</sup>Southern University of Science and Technology, Shenzhen, China

<sup>7</sup>Department of Geology and Geophysics, Woods Hole Oceanographic Institution, Woods Hole, Massachusetts, USA

## Correspondence

Fan Zhang, Key Laboratory of Ocean and Marginal Sea Geology, South China Sea Institute of Oceanology, Innovation Academy of South China Sea Ecology and Environmental Engineering, Chinese Academy of Sciences, Guangzhou, China.  
Email: zhangfan@scsio.ac.cn

## Funding information

Southern Marine Science and Engineering Guangdong Laboratory (Guangzhou), Grant/Award Number: GML2019ZD0205; NSFC, Grant/Award Number: 41976064, 91958211, 41706056 and 41890813; Chinese Academy of Sciences, Grant/Award Number: Y4SL021001, QYZDY-SSW-DQC005 and 133244KYSB20180029; Hong Kong Research Grant Council, Grant/Award Number: 14304820 and 14306119

## Abstract

The influence of subducting plateaux on inter-plate earthquakes has been extensively studied. However, its effects on plate bending, stress distribution and intra-plate earthquakes remain unclear. Here we model the deflection of a subducting oceanic plate with an oceanic plateau regarded as a high flexure rigidity body near the trench using a thin plate model. Dozens of models were carried out to study the effects of the distance between plateau and trench on flexural bending and stress with variable flexural rigidity. We find that the influence of plateau depends on its location with respect to the trench axis and it begins to affect the plate bending when its distance from the trench axis is ~70–120 km. It changes the bending stress distribution and causes concentrated deformation to the trench-ward of the plateau. After the plateau starts to subduct, pre-existing bending faults may be reactivated by the differential forces caused by the lateral variation in slab buoyancy between the shallower seamounts/plateaus and the deeper slab.

## KEYWORDS

bending stress, intra-plate earthquakes, plate bending, plateau, subduction zone

## 1 | INTRODUCTION

Oceanic plateaux classified as large igneous provinces are commonly thought to derive from ascending mantle plumes (Coffin

& Eldholm, 1993, 1994; Eldholm & Coffin, 2000; Taylor, 2006). Plateau/seamount subduction has been observed at different trenches, such as the Amami Plateau at the Ryukyu Trench, the Caroline ridge and numerous seamounts at the Southern Mariana

Trench (Figure 1), the Hikurangi plateau in the north New Zealand subduction zone (Herath et al., 2020), and the Yakutat plateau in the Alaska subduction zone (Worthington et al., 2012). The influences of plateau or seamount subduction on inter-plate seismicity at subduction zone have been widely investigated (Bell et al., 2014; Gao & Wang, 2014; Geersen et al., 2015; Kodaira et al., 2000; Mochizuki et al., 2008; Ruh et al., 2016; Sallares et al., 2013; Singh et al., 2011; Yang et al., 2012, 2013). However, the impacts of plateaux on subducting plate bending, stress state and intraplate earthquakes have been rarely studied.

Plate bending may cause active trench-parallel normal faulting, providing important pathways for seawater to hydrate the incoming plate (e.g., Cabrera et al., 2021; Cai et al., 2018; Zhang et al., 2021; Zhou et al., 2015; Zhu et al., 2021) and generating tensional earthquakes at outer rise. A thin plate model was most often used to investigate the plate deflection and bending stress, and the corresponding outer rise intraplate earthquakes (Garcia-Castellanos et al., 2000; Watts, 2001; Contreras-Reyes & Osses, 2010; Emry et al., 2014; Zhou et al., 2015, 2018; Zhou & Lin, 2018; Zhang et al., 2014; Zhang et al., 2018). Based on the thin plate model, the deflection of subducting plate is determined by the trench axis loading and the flexural rigidity or the effective elastic thickness ( $T_e$ ) of the plate (Turcotte & Schubert, 2014). In previous studies, the  $T_e$  of subducting plate was regarded as a constant at the area seaward of the outer rise and decreased with the distance from the trench axis due to inelastic deformation (Contreras-Reyes & Osses, 2010). The swell topographies of the oceanic plateau obscure the outer rise signature and make more complicated to isolate the signature caused by plate bending (Contreras-Reyes et al., 2019, 2021).

Recent works reported that the subducted plateaux can modify the patterns of plate bending deformation and bending-related earthquakes (Arai et al., 2017; Herath et al., 2020; Shulgin et al., 2011) (Figure 2). Here, we used a simple thin plate flexural model to investigate the effects of incoming plateau near the outer rise region on the plate flexure, bending stress and the corresponding intraplate seismicity. We finally proposed a mechanism to explain the observed faulting near the outer rise region at the Ryukyu and the Java subduction zones.

## 2 | METHOD AND MODEL SETUP

### 2.1 | Method

Here, we simulated the plate deflection by a variable-thickness elastic cantilever beam on Winkler basement (Figure 3). The deflection  $w$  of the plate can be described as (Turcotte & Schubert, 2014).

$$-\frac{d^2}{dx^2} \left( D \frac{d^2 w}{dx^2} \right) + \frac{d}{dx} \left( F \frac{dw}{dx} \right) + (\rho_m - \rho_w) w g = q(x). \quad (1)$$

where  $F$  is the horizontal force which is set to zero in our model.  $\rho_m$  and  $\rho_w$  represent the densities of mantle and seawater, respectively.  $q(x)$  is the overlying load.  $D$  is the flexure rigidity of lithosphere given by

### Statement of significance

Subduction of oceanic plateaux is quite common. However, the effect of plateau subduction on lithospheric deformation and seismicity at subduction zones is unclear. In this study, we use 2-D plate bending model to tackle two issues. First, we quantify the plateau subduction effect on lithospheric deformation. Second, we investigate the influence of a subducting plateau on seismicity at subduction zones. Our results show that subducting plateau can cause concentration of bending stress and may enhance intraplate seismicity.

$D = \frac{ET_e^3}{12(1-\mu^2)}$ , where  $E$  is the Young's modulus,  $\mu$  is the Poisson's ratio and  $T_e$  is the effective elastic thickness (Please see Table S1).

Once the plate deflection  $w$  is obtained, the plate bending stress ( $\sigma$ ) can be calculated by  $\sigma = \frac{E}{1-\mu^2} \frac{d^2 w}{dx^2} z$ , where  $z$  is the distance from the neutral plane of the plate. Considering the yield strength of the lithosphere, we corrected the bending stress by the lithospheric yield strength envelope (YSE), to constrain the region where earthquakes may happen (Figure 3b,c). Combination of Coulomb-Navier failure criterion at shallow parts (Byerlee, 1978; Goetze & Evans, 1979) and two ductile flow laws at deeper parts (Hirth & Kohlstedt, 2003; Mei et al., 2010) were adopted in this study (The strain rate is  $10^{-16} \text{ s}^{-1}$  as same as in Hunter & Watts, 2016) (Figure 3c). We assume that the oceanic plateau has different  $T_e$  with surrounding normal oceanic plate which affects the plate curvature and the bending stress.

### 2.2 | Model setup

Bathymetry data show that the general scales of plateaux near trenches are ~160 to ~400 km (Figure S1 and S2). Meanwhile, Hunter and Watts (2016) point out that the short profile omits much of the flexural signal and suggested length of model larger than 500 km. Therefore, the lengths of modelled subducting plate ( $L$ ) and plateau ( $L_p$ ) are 700 and 300 km, respectively.  $x_p$  represents the distance from the trench-ward edge of the plateau to the trench axis. (Figure 3a). We mainly focused on the effects of  $x_p$  and  $T_e$  of oceanic plate on the deflection and bending stress. The bending moment ( $M_0$ ) and shear force ( $V_0$ ) are set to  $2 \times 10^{16} \text{ Nm}$  and  $1 \times 10^{12} \text{ N}$ , respectively, which are usual values at the trench axis (Hunter & Watts, 2016; Zhang et al., 2020). The  $\sigma_m$  means maximum bending stress and the  $d_y$  means the maximum depth of the yield zone (Figure 3d). The  $x_{tm}$  and the  $x_{pm}$  represent the distance between the location of  $\sigma_m$  with trench axis and plateau, respectively.

In order to test the influence of an approaching plateau on plate bending, the  $T_e$  of the plateau is set to be larger than, equal to and smaller than that of normal oceanic plate, respectively (Figure S3). We find that if the  $T_e$  of plateau is smaller than that of normal subducting plate, the height of plate forebulge increases (Green line in

**FIGURE 1** Subducting plateaus near different trenches (red areas). (a) Plateaus near the Izu-Bonin, the Mariana, the Philippine and the Ryukyu Trenches (red areas). The magenta line (profile a) is a seismic profile from Arai et al. (2017) displayed in the Figure 2a. (b) The Roo Rise Plateau near the Java Trench. The magenta line (profile b) is a seismic profile from Shulgin et al. (2011) displayed in Figure 2b

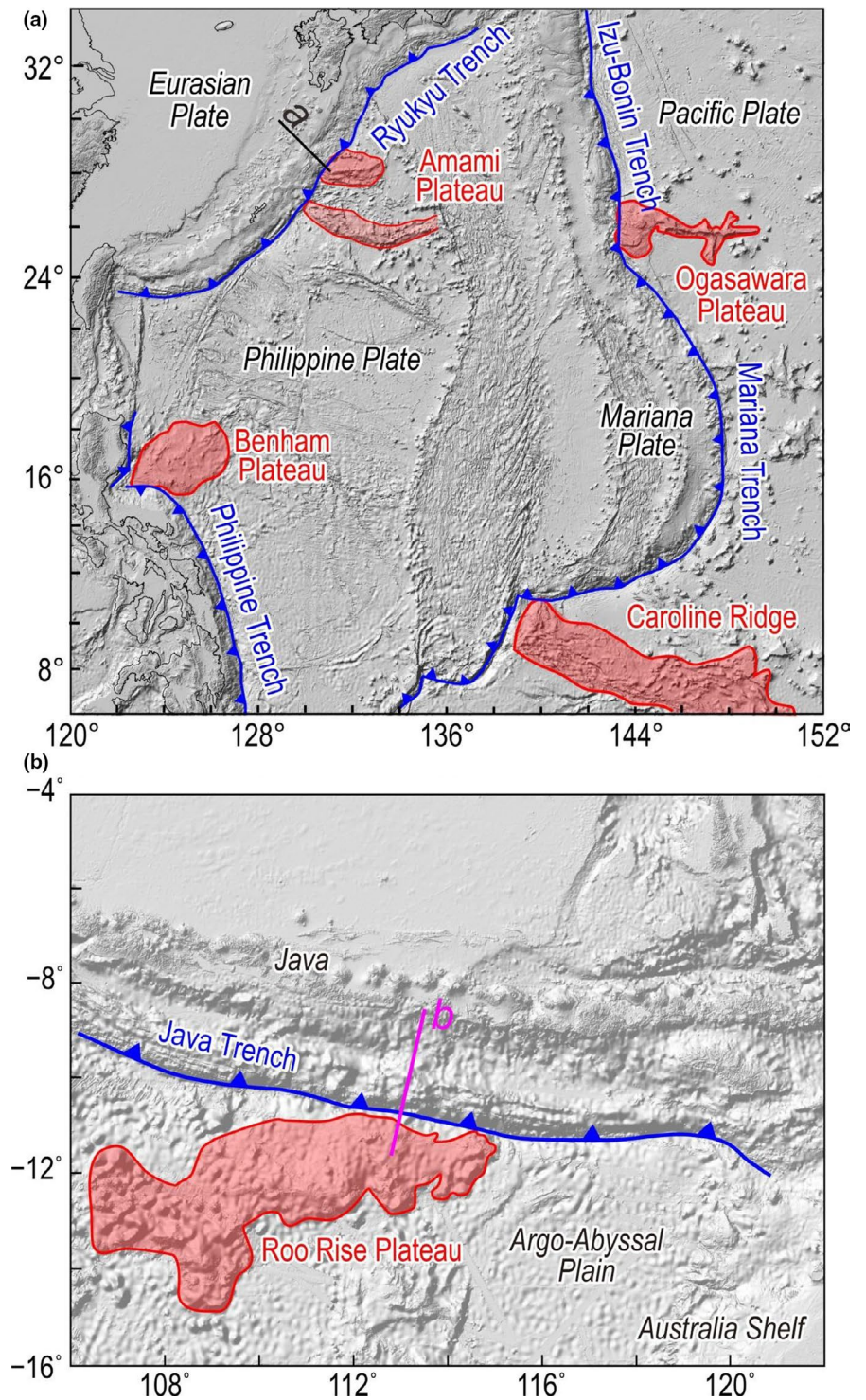
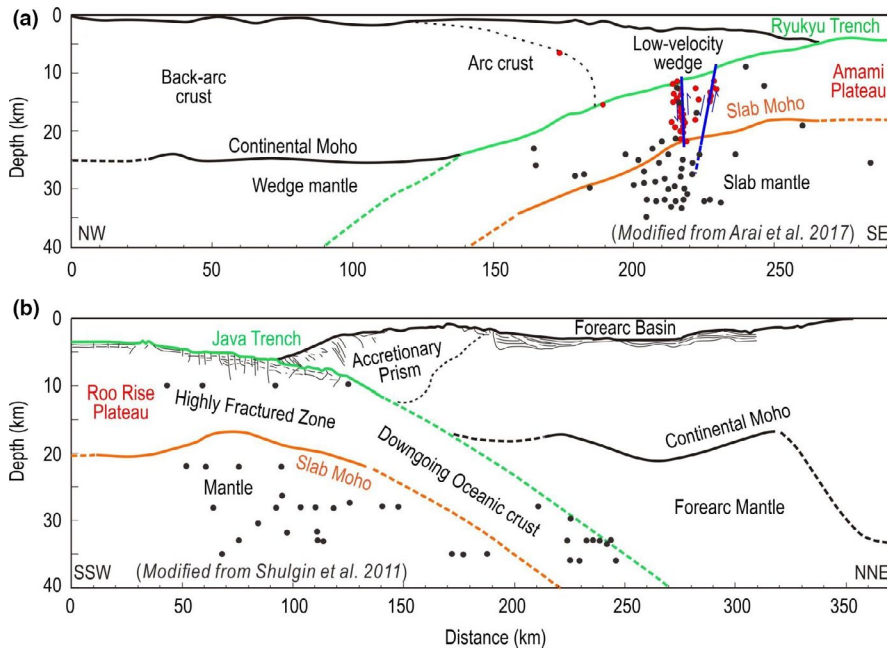
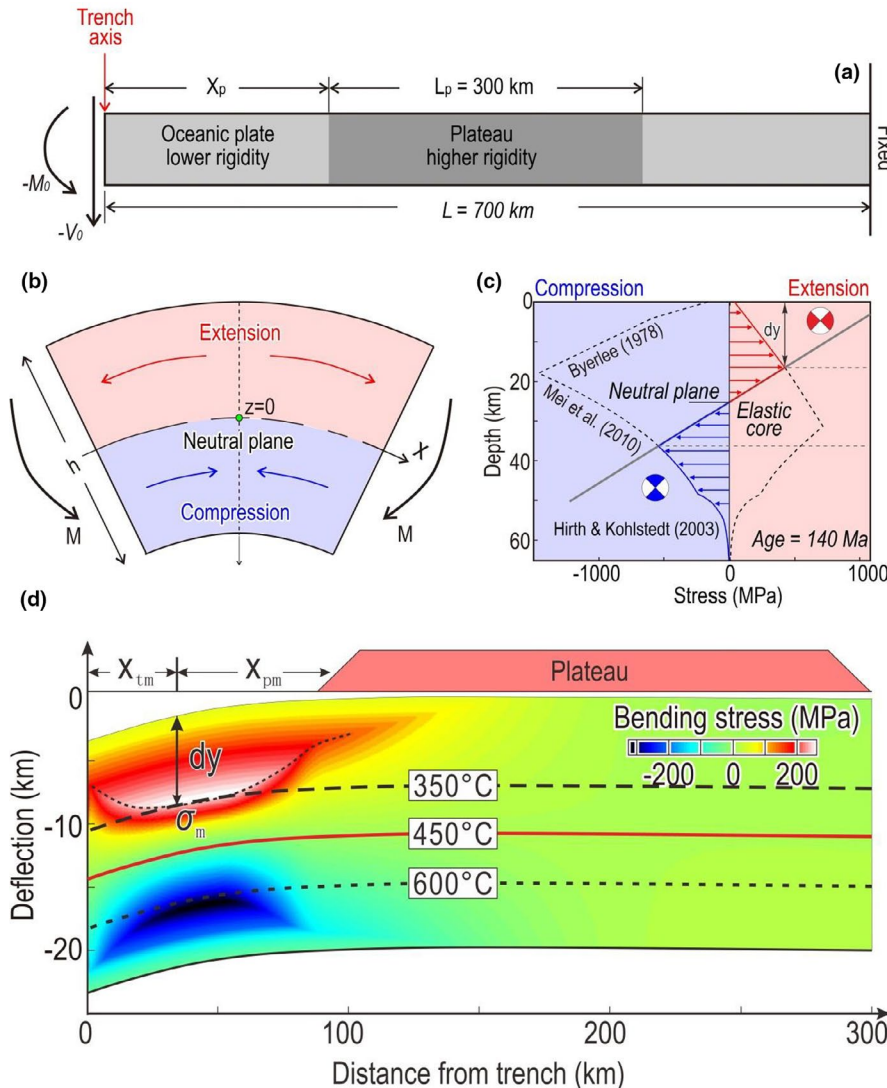


Figure S3a) and the plate curvature reaches maximum at the plateau (Green dashed line in Figure S3b). In contrast, if the plateau has a larger  $T_e$ , the height of plate forebulge plate decreases (Red line in Figure S3a), and the plate curvature reaches a maximum in front of the plateau (Red dashed line in Figure S3b). By considering the dependence of  $T_e$  on the square root of plate age (Hunter & Watts, 2006) and the fact that the plateau is no older than the oceanic lithosphere (Calmant et al., 1990), the  $T_e$  of plateau should be smaller than that of oceanic plate. However, highly fractured

zone observed in front of the subducting plateau (Figure 2b) and the fact that fewer bending-related faults and earthquakes (Mochizuki et al., 2008) were found within the subducting plateau larger than about 40 km (Fryer & Smoot, 1985) seem to suggest that the plateau has higher  $T_e$  than normal oceanic plate. Therefore, the  $T_e$  of plateau is set to 10 km thicker than that of normal oceanic plate. Here we did not consider the influence of plateau on the plate bending topography and so we did not try to separate the swell topography of plateau from the outer rise like Contreras-Reyes et al. (2021).



**FIGURE 2** Geological structures along the profile a (Figure 1a) crossing the Ryukyu Trench (from Arai et al., 2017) and the profile b (Figure 1b) crossing the Java Trench (from Shulgin et al., 2011). The red dots represent the relocated aftershocks of the 1995 events occurred in the Java trench (Arai et al., 2017). The black dots are earthquakes occurred in subducting plate since 1990 (within a 10-km-wide box on both sides along the profile for hypocenter projection) (from the International Seismological Centre)



**FIGURE 3** (a) Model setup. The bending moment  $-M_0$  and the vertical shear force  $-V_0$  are loadings applied at trench axis. The far end is fixed.  $L$  and  $L_p$  are the lengths of modeled subducting plate and plateau, respectively.  $x_p$  represents the distance between the plateau and the trench axis. Dark and light gray areas show subducting plate with and without plateau, respectively. (b) Schematic of extension (pink area) and compression (pale blue area) at the upper and lower plate caused by plate bending. Dashed line represents the neutral plane of the plate.  $z$  is the distance from the neutral plane of plate. (c) Yield strength envelop of plate. The blue and red curves represent the yield strength envelope (YSE) and the gray line shows the slope of the elastic core. Combination of Coulomb-Navier failure criterion at shallow part (Byerlee, 1978; Goetze & Evans, 1979) and two ductile flow laws at deeper part (Hirth & Kohlstedt, 2003; Mei et al., 2010) is adopted in this study. (d) Bending stress distribution in a subducting plate. Pink area is the location of plateau. Black dashed line marks the calculated yield zone.  $d_y$  means the depth of yield zone.  $s_m$  means the maximum bending stress.  $x_{tm}$  and  $x_{pm}$  are the distance of the location of  $s_m$  from trench and plateau, respectively. The black dashed, red solid and black dotted lines are the 350, 450 and 600°C isotherms, respectively, based on the semi-infinite half-space cooling model

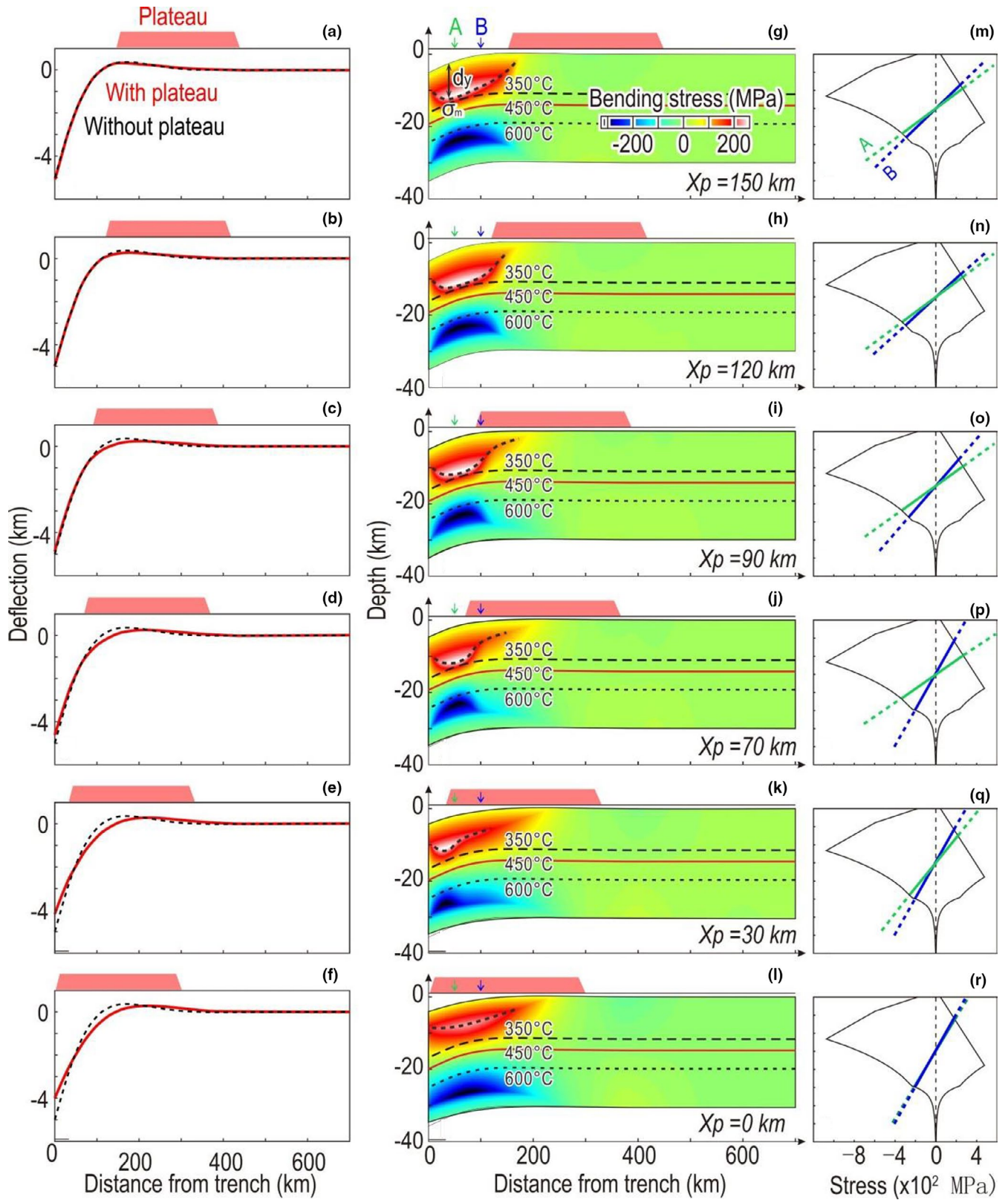
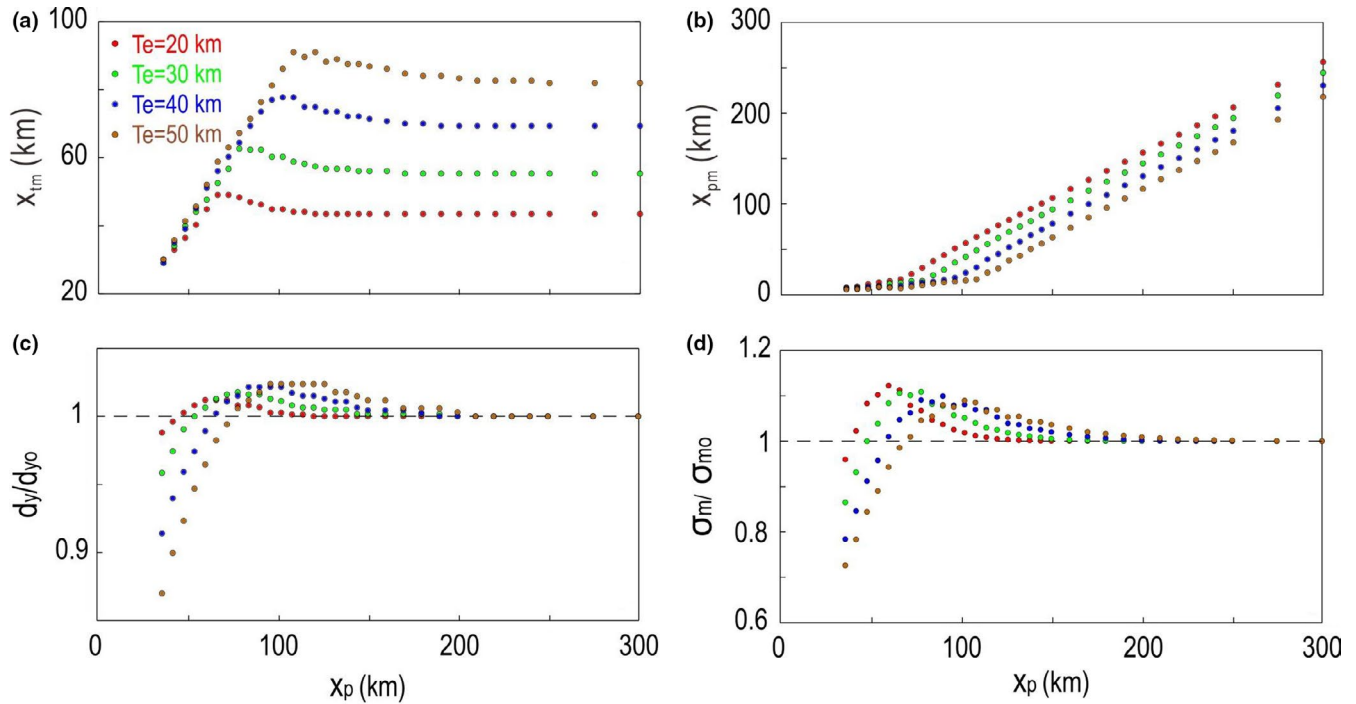


FIGURE 4 (a–f) Plate deflection with the distance between plateau and trench is 150–0 km, respectively. Pink area marks the location of plateau. Red solid and black dashed lines are the plate deflection with and without plateau under the same loadings, respectively. (g–l) Plate bending stress with the distance between plateau and trench is 150–0 km, respectively. (m–r) Example slopes of plate elastic core for locations of 50 km (the green arrow in the panel g) and 100 km (the blue arrow in the panel g) from the trench axis. The black dashed, red solid and black dotted lines are the 350, 450 and 600°C isotherms, respectively, based on the semi-infinite half-space cooling model



**FIGURE 5** The correlations of the distance between the plateau and trench  $x_p$  and location of maximum bending stress ( $s_m$ ) and yield zone depth ( $d_y$ ) with different  $T_e$ . (a) The relationship between  $x_p$  and the distance between the location of  $\sigma_m$  and the trench axis ( $x_{tm}$ ). It shows that  $x_{tm}$  first increase and then decrease with the decrease of  $x_p$ . The maximum value of  $x_{tm}$  increases with  $T_e$  which means that the influence range of plateaus on strong plate is larger than that of weak plate. (b) The relationship between  $x_p$  and the distance between the location of  $\sigma_m$  and the plateau ( $x_{pm}$ ). It shows that  $x_{pm}$  is linearly correlated with  $x_p$  when the plateau is far away from the trench axis and keeps in 15–25 km when the plateau closes to trench axis. (c) The relationship between  $x_p$  and  $d_y$ . (d) The relationship between  $x_p$  and the magnitude of  $\sigma_m$ . All models are under the same boundary loadings ( $M_0 = 2 \times 10^{16}$  Nm and  $V_0 = 1 \times 10^{12}$  N)

### 3 | RESULTS

Firstly, we conducted a test model with constant boundary loading and  $T_e$ . The independent variable is  $x_p$  (Figure 4). We find that under the fix boundary loading and  $T_e$  ( $T_e = 20$  km in Figure 4), the plate deformation was strongly controlled by the distance between the plateau and the trench axis. When the plateau is far away from the trench axis ( $x_p = 120$ – $150$  km in Figure 4a,b), it has little influence on plate deflection; when the plateau is close to the trench, the bulge of plate become gentle and the bending deformation of plate is concentrated in front of the plateau ( $x_p = 70$ – $90$  km in Figure 4c,d). With further decrease of  $x_p$ , the plate deflection becomes smaller than that of normal oceanic plate (Figure 4e,f), the stress distribution becomes more concentrated (Figure 4j–l) and the yield zone becomes narrower and shallower (Dashed lines in Figure 4j–l and Figure 4q,r). The neutral plane follows the 450°C isotherms roughly (Carrasco et al., 2019; Ruiz & Contreras-Reyes, 2015; Seno & Yamanaka, 1996) (Figures 3d and 4).

Secondly, hundreds of models were carried out to study the effects of plateau subduction on plate bending and stress distribution under variable  $x_p$  changes from 300 to 36 km (The distance similar to Shulgin et al., 2011), as well as the normal oceanic plate  $T_e$  of 20, 30, 40 and 50 km, respectively (Table S2 and Figure 5). It shows that the  $x_{tm}$  increases with  $T_e$  under the same boundary

loading (Figure 5a). The impact of  $x_p$  on  $x_{tm}$  also depends on the  $T_e$ . When  $T_e$  is 50 km, the influence of plateau on the  $x_{tm}$  becomes apparent when the  $x_p$  decreases to  $\sim 120$  km. However, if the  $T_e$  is 20 km, the influence of plateau starts to become obvious when  $x_p$  is  $\sim 70$  km (Figure 5a). The  $x_{pm}$  is also related to the  $x_p$ . When the plateau is far away from the trench, the  $x_p$  and the  $x_{pm}$  are linearly correlated. However, when the plateau is a certain distance from the trench, i.e.,  $x_p$  decreases to  $\sim 120$  km ( $T_e = 50$  km) or  $\sim 70$  km ( $T_e = 20$  km), the  $x_{pm}$  is no longer correlated to the  $x_p$  and keeps in 15–25 km (Figure 5b).

The magnitude of  $\sigma_m$  first increases and then decreases with the decrease of  $x_p$  (Figure 5d), and the  $d_y$  shows the similar trend (Figure 5c). The increase and decrease in  $d_y$  are 2%–3% and 5%–14%, respectively. The increase and decrease in  $\sigma_m$  are 10% and 5%–25%, respectively. Please note that both  $\sigma_m$  and  $d_y$  are normalized by the original values that are not influenced by plateau ( $\sigma_{m0}$  and  $d_{y0}$ ).

### 4 | DISCUSSION

Our models suggest that when the plateau approaches the trench axis, the yield zone would highly concentrate on the front of plateau, which fits the observations well. Using wide-angle

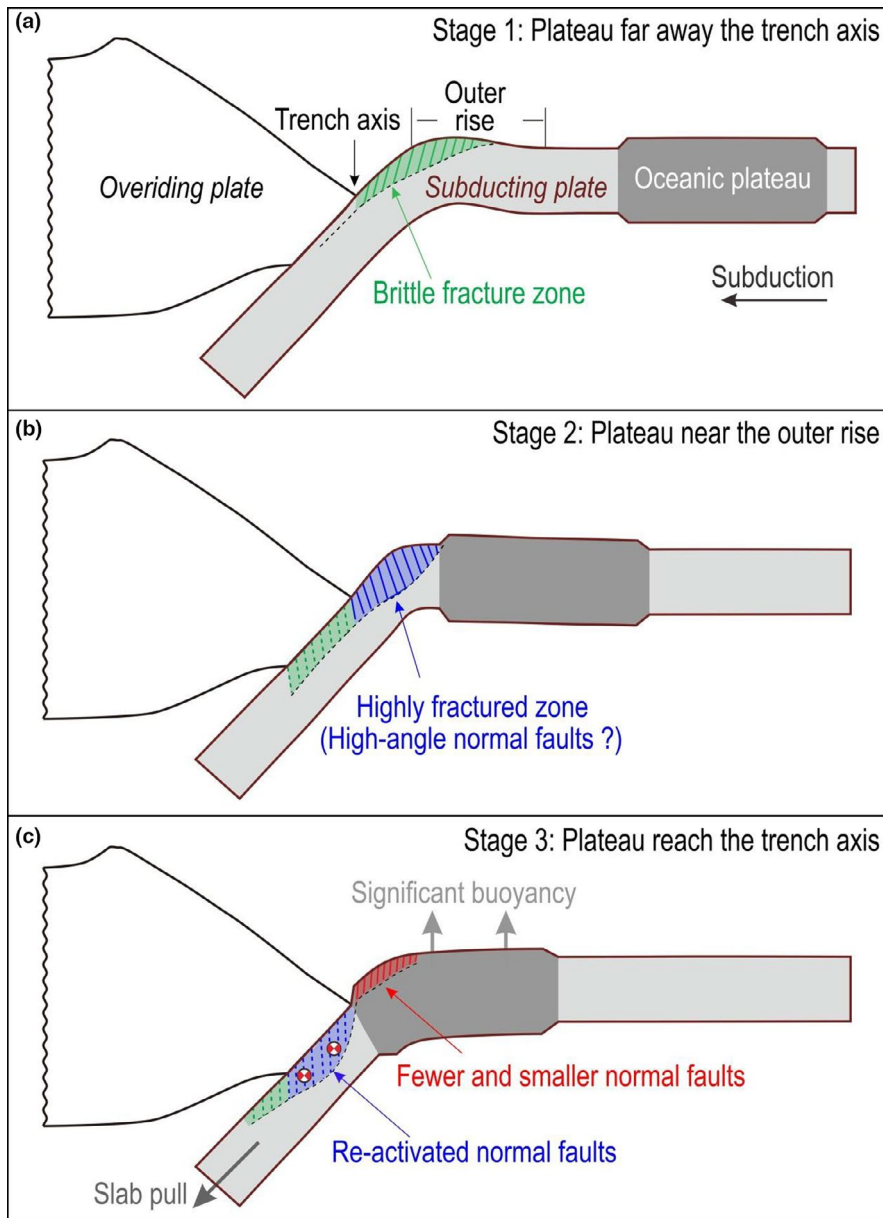


**FIGURE 6** Illustration of effects of plateau subduction on plate bending, stress and intraplate seismicity. (a) Plate bending and brittle yield zone (green stripes) of a subducting plate with a plateau far away from the trench axis. (b) Stresses are concentrated and a highly fracture zone (blue stripes) is formed on the front of plateau when it is close to the outer rise. (c) When the plateau reaches the trench axis, the subducting plate is associated with shallower yield zone, fewer and smaller normal faults (red stripes). The subducted normal faults are re-activated (blue dashed lines)

seismic data, Shulgin et al. (2011) investigated the structural architecture of the Roo Rise oceanic plateau at the Java subduction zone. They found a highly fractured zone developed in the front the plateau, whereas only few faults were observed with the plateau itself (Figure 2b). It means that the strength heterogeneity of the subducting plate may make the deformation concentrate in the front of plateau and increase the depths of yield zone and bending-related earthquakes. The swell of oceanic plateau also plays a crucial role on intraplate seismicity. Contreras-Reyes and Carrizo (2011) proposed that subducting plateau plays double roles in earthquake rupture: acting as barriers or asperities. It mainly depends on the interplay between the yield shear stress near the subducting high feature and the energy carried by the rupture front. Also at Java trench, the subducting Roo Rise plateau may lead to locally locked patches on an otherwise decoupled, aseismic slipping subduction zone,

causing the 1994 Java tsunami earthquake (Abercrombie et al., 2001).

When plateaux reach the trench axis or just start to subduct, the buoyancy begins to play a major role on plate deformation and intraplate earthquakes. Seismic studies in the Ryukyu Trench (Arai et al., 2017) showed high-angle normal faults and along-fault-plane earthquakes in front of a subducting seamount (Figure 2a). Arai et al. (2017) suggested that these high-angle normal faults (dip angle of 70–80°) may be caused by the significant buoyancy of seamount or plateau rather than the bending faults of which the dip angles are moderate (Craig et al., 2014). Here, we propose another possible mechanism for these high-angle normal-fault events. These high-angle normal faults may be inherited by bending faults that had formed before and be reactivated by the tensional stress coming from the differential buoyancy between the plateau and the deeper slab. We infer that the extreme high plate curvature concentrated in

the front of plateau (corresponding to the high fracture zone) may be related to the formation of high-angle normal faults. Besides, the distance between the high-angle normal faults and seamount is ~20 km (Figure S2a) which is coincident with the distance between plateau and  $\sigma_m$ . We therefore speculate that these high-angles were caused by plate bending in the highly fractured zone ahead of seamount/plateau. Intraplate earthquakes are also observed to be concentrated beneath the subduction front of the seamount in the Japan Trench (Mochizuki et al., 2008). It is therefore a widespread phenomenon. Furthermore, Chesley et al. (2020) reported a prominent, sub-vertical low resistivity zone in front of a subducting seamount at the northern Hikurangi Margin. The low resistivity zone corresponds to a normal fault, indicating that the fault is probably a porous conduit for fluid flow. We infer that the low resistivity zone may reflect the enhanced hydration of subducting plate caused by plateau subduction.

Based on the above discussion, we propose a model to illustrate the effects of plateau subduction on plate bending, stress and seismicity (Figure 6). Subduction of oceanic plateau would induce different geological phenomena at different stages. When the plateau is far away from the trench, it has little influence on plate bending, the brittle yield zone and the bending-related normal faulting (Figure 6a). As the plateau approaching the trench, it plays a major role in plate deflection. The heterogeneity of subduction plate can cause the concentrated flexure deformation, as well as the highly fractured zone, at the front of the plateau (Figure 6b). When the plateau finally reaches the trench, the lateral variation in slab buoyancy between the shallower seamounts/plateaus and the deeper slab may cause different force and reactivation of pre-existing bending faults (Figure 6c).

Both plateaux and trenches have very complicated geometry. This would bring three dimensional effects which may affect dramatically the plate stress state. We infer that the incoming plateau would cause the lateral flexure along the strike of the trench (Contreras-Reyes et al., 2021; Zhang, Sun, et al., 2018).

## 5 | CONCLUSIONS

Bending deformation concentrates in front of plateaux at the outer rise which may cause highly fractured zone. The impacts of plateau subduction on plate deformation, bending stress and yield zone depth mainly rely on the distance between the plateau and the trench axis and the rigidity of subducting plate. The influences begin to appear when the plateau is ~70 km (on a weak plate) to ~120 km (on a strong plate) away from the trench axis. At this stage, the concentrated flexure deformation and the highly fractured zone develop in front of plateau with the maximum bending stress 15–25 km ahead of the plateau. With the plateau a close to the trench axis, both bending stress and yield zone depth first increase and then decrease. After the plateau enters the subduction zone, the bending faults may be reactivated by the extensional stress from

differential buoyancies between the plateau and deeper slab. Thus, intraplate earthquakes may be concentrated in front of the subducting plateau.

## ACKNOWLEDGEMENTS

This research benefited from discussion with the SCSIO Marine Geodynamics Group. This work was supported by Southern Marine Science and Engineering Guangdong Laboratory (Guangzhou) grants GML2019ZD0205; NSFC grants 41976064, 91958211, 41706056, and 41890813; the Chinese Academy of Sciences grants Y4SL021001, QYZDY-SSW-DQC005, and 133244KYSB20180029; Hong Kong Research Grant Council Grants (No. 14304820, 14306119), Faculty of Science at CUHK.

## DATA AVAILABILITY STATEMENT

Data sharing is not applicable to this article as no new data were created or analysed in this study.

## REFERENCES

- Abercrombie, R. E., Antolik, M., Felzer, K., & Ekström, G. (2001). The 1994 Java tsunami earthquake: Slip over a subducting seamount. *Journal of Geophysical Research*, 106(B4), 6595–6607. <https://doi.org/10.1029/2000JB900403>
- Arai, R., Kodaira, S., Yamada, T., Takahashi, T., Miura, S., Kaneda, Y., Nishizawa, A., & Oikawa, M. (2017). Subduction of thick oceanic plateau and high-angle normal-fault earthquakes intersecting the slab. *Geophysical Research Letters*, 44, 6109–6115. <https://doi.org/10.1002/2017GL073789>
- Bell, R., Holden, C., Power, W., Wang, X. M., & Downes, G. (2014). Hikurangi margin tsunami earthquake generated by slow seismic rupture over a subducted seamount. *Earth and Planetary Science Letters*, 397, 1–9.
- Byerlee, J. (1978). Friction of rocks. *Pure and Applied Geophysics PAGEOPH*, 116(4–5), 615–626. <https://doi.org/10.1007/BF00876528>
- Cabrera, L., Ruiz, S., Poli, P., Contreras-Reyes, E., Osses, A., & Mancini, R. (2021). Northern Chile intermediate-depth earthquakes controlled by plate hydration. *Geophysical Journal International*, 226(1), 78–90. <https://doi.org/10.1093/gji/ggaa565>
- Cai, C., Wiens, D. A., Shen, W., & Eimer, M. (2018). Water input into the Mariana subduction zone estimated from ocean-bottom seismic data. *Nature*, 563, 389–392. <https://doi.org/10.1038/s41586-018-0655-4>
- Calmant, S., Francheteau, J., & Cazenave, A. (1990). Elastic layer thickening with age of the oceanic lithosphere: A tool for prediction of the age of volcanoes or oceanic crust. *Geophysical Journal International*, 100(1), 59–67. <https://doi.org/10.1111/j.1365-246X.1990.tb04567.x>
- Carrasco, S., Ruiz, J. A., Contreras-Reyes, E., & Ortega-Culaciati, F. (2019). Shallow intraplate seismicity related to the Illapel 2015 Mw 8.4 earthquake: Implications from the seismic source. *Tectonophysics*, 766, 205–218.
- Chesley, C., Nail, S., Key, K., & Bassett, D. (2020). Fluid-rich subducting topography generates anomalous forearc porosity. *Nature*, 595, 255–260. <https://doi.org/10.1038/s41586-021-03619-8>
- Coffin, M. F., & Eldholm, O. (1993). Scratching the surface: Estimating dimensions of large igneous provinces. *Geology*, 21(6), 515–518. [https://doi.org/10.1130/0091-7613\(1993\)021<0515:STSED>2.3.CO;2](https://doi.org/10.1130/0091-7613(1993)021<0515:STSED>2.3.CO;2)
- Coffin, M. F., & Eldholm, O. (1994). Large igneous provinces: Crustal structure, dimensions, and external consequences. *Reviews of Geophysics*, 32(1), 1–36. <https://doi.org/10.1029/93RG02508>

- Contreras-Reyes, E., & Carrizo, D. (2011). Control of high oceanic features and subduction channel on earthquake ruptures along the Chile-Peru subduction zone. *Physics of the Earth and Planetary Interiors*, 186, 49–58. <https://doi.org/10.1016/j.pepi.2011.03.002>
- Contreras-Reyes, E., Cortés-Rivas, V., Manríquez, P., & Maksymowicz, A. (2021). The silent bending of the oceanic Nazca Plate at the Peruvian Trench. *Tectonophysics*, 807, 228810. <https://doi.org/10.1016/j.tecto.2021.228810>
- Contreras-Reyes, E., Muñoz-Linford, P., Cortes-Rivas, V., Bello, J. P., Ruiz, J. A., & Krabbenhoef, A. (2019). Structure of the collision zone between the Nazca Ridge and the Peruvian convergent margin: Geodynamic and seismotectonic implications. *Tectonics*, 38(9), 3416–3435. <https://doi.org/10.1029/2019TC005637>
- Contreras-Reyes, E., & Osses, A. (2010). Lithospheric flexure modelling seaward of the Chile trench: Implications for oceanic plate weakening in the Trench Outer Rise region. *Geophysical Journal International*, 182(1), 97–112. <https://doi.org/10.1111/j.1365-246X.2010.04629.x>
- Craig, T. J., Copley, A., & Jackson, J. (2014). A reassessment of outer-rise seismicity and its implications for the mechanics of oceanic lithosphere. *Geophysical Journal International*, 197(1), 63–89. <https://doi.org/10.1093/gji/ggu013>
- Eldholm, O., & Coffin, M. F. (2000). Large igneous provinces and plate tectonics. In M. A. Richards, R. G. Gordon, & R. D. van der Hilst (Eds.), *The history and dynamics of global plate motions* (pp. 309–326). American Geophysical Union.
- Emry, E. L., Wiens, D. A., & Garcia-Castellanos, D. (2014). Faulting within the Pacific plate at the Mariana Trench: Implications for plate interface coupling and subduction of hydrous minerals. *Journal of Geophysical Research: Solid Earth*, 119, 2076–3095. <https://doi.org/10.1002/2013JB010718>
- Fryer, P., & Smoot, N. C. (1985). Processes of seamount subduction in the Mariana and Izu-Bonin trenches. *Marine Geology*, 64, 7–90. [https://doi.org/10.1016/0025-3227\(85\)90161-6](https://doi.org/10.1016/0025-3227(85)90161-6)
- Gao, X., & Wang, K. L. (2014). Strength of stick-slip and creeping subduction megathrusts from heat flow observations. *Science*, 345(6200), 1038–1041.
- García-Castellanos, D., Torne, M., & Fernandez, M. (2000). Slab pull effects from a flexural analysis of the Tonga and Kermadec trenches (Pacific Plate). *Geophysical Journal International*, 141(2), 479–484. <https://doi.org/10.1046/j.1365-246x.2000.00096.x>
- Geersen, J., Ranero, C. R., Barckhausen, U., & Reichert, C. (2015). Subducting seamounts control interplate coupling and seismic rupture in the 2014 Iquique earthquake area. *Nature Communications*, 6, 8267. <https://doi.org/10.1038/ncomms9267>
- Goetze, C., & Evans, B. (1979). Stress and temperature in the bending lithosphere as constrained by experimental rock mechanics. *Geophysical Journal International*, 59(3), 463–478.
- Herath, P., Stern, T. A., Savage, M. K., Bassett, D., Henrys, S., & Boulton, C. (2020). Hydration of the crust and upper mantle of the Hikurangi Plateau as it subducts at the southern Hikurangi margin. *Earth and Planetary Science Letters*, 541, 116271. <https://doi.org/10.1016/j.epsl.2020.116271>
- Hirth, G., & Kohlstedt, D. (2003). Rheology of the upper mantle and the mantle wedge: A view from the experimentalists. In J. Eiler (Ed.), *Inside the subduction factory* (pp. 83–105). American Geophysical Union.
- Hunter, J., & Watts, A. B. (2016). Gravity anomalies, flexure and mantle rheology seaward of circum-Pacific trenches. *Geophysical Journal International*, 207(1), 288–316. <https://doi.org/10.1093/gji/ggw275>
- Kodaira, S., Takahashi, N., Nakanishi, A., Miura, S., & Kaneda, Y. (2000). Subducted seamount imaged in the rupture zone of the 1946 Nankaido earthquake. *Science*, 289, 104–106. <https://doi.org/10.1126/science.289.5476.104>
- Mei, S., Suzuki, A. M., Kohlstedt, D. L., Dixon, N. A., & Durham, W. B. (2010). Experimental constraints on the strength of the lithospheric mantle. *Journal of Geophysical Research*, 115(B8). <https://doi.org/10.1029/2009JB006873>
- Mochizuki, K., Yamada, T., Shinohara, M., Yamanaka, Y., & Kanazawa, T. (2008). Weak interplate coupling by seamounts and repeating M similar to 7 earthquakes. *Science*, 321(5893), 1194–1197.
- Ruh, J. B., Sallarès, V., Ranero, C. R., & Gerya, T. (2016). Crustal deformation dynamics and stress evolution during seamount subduction: High-resolution 3-D numerical modeling. *Journal of Geophysical Research: Solid Earth*, 121, 6880–6902.
- Ruiz, J., & Contreras-Reyes, E. (2015). Outer rise seismicity boosted by the Maule 2010 Mw 8.8 megathrust earthquake. *Tectonophysics*, 653, 127–139. <https://doi.org/10.1016/j.tecto.2015.04.007>
- Sallares, V., Melendez, A., Prada, M., Ranero, C. R., McIntosh, K., & Grevemeyer, I. (2013). Overriding plate structure of the Nicaragua convergent margin: Relationship to the seismogenic zone of the 1992 tsunami earthquake. *Geochemistry, Geophysics, Geosystems*, 14, 3436–3461. <https://doi.org/10.1002/ggge.20214>
- Seno, T., & Yamanaka, Y. (1996). In G. E. Bebout, D. W. Scholl, S. H. Kirby, & J. P. Platt (Eds.), *Double seismic zones, compressional deep trench-outer rise events, and superplumes, in subduction: Top to Bottom*, (96, pp. 347–355). American Geophysical Union.
- Shulgin, A., Kopp, H., Mueller, C., Planert, L., Lueschen, E., Flueh, E. R., & Djajadihardja, Y. (2011). Structural architecture of oceanic plateau subduction offshore Eastern Java and the potential implications for geohazards. *Geophysical Journal International*, 184, 12–28. <https://doi.org/10.1111/j.1365-246X.2010.04834.x>
- Singh, S. C., Hananto, N., Mukti, M., Robinson, D. P., Das, S., Chauhan, A., Carton, H., Gratacos, B., Midnet, S., Djajadihardja, Y., & Harjono, H. (2011). Aseismic zone and earthquake segmentation associated with a deep subducted seamount in Sumatra. *Nature Geoscience*, 4(5), 308–311.
- Taylor, B. (2006). The single largest oceanic plateau: Ontong Java-Manihiki-Hikurangi. *Earth and Planetary Science Letters*, 241, 372–380. <https://doi.org/10.1016/j.epsl.2005.11.049>
- Turcotte, D., & Schubert, G. (2014). *Geodynamics*, 3rd ed. (p. 626). Cambridge University Press.
- Watts, A. B. (2001). *Isostasy and flexure of the lithosphere*, 1st ed. (p. 478). Cambridge University Press.
- Worthington, L. L., Van Avendonk, H. J. A., Gulick, S. P. S., Christeson, G. L., & Pavlis, T. L. (2012). Crustal structure of the Yakutat Terrane and the evolution of subduction and collision in southern Alaska. *Journal of Geophysical Research: Solid Earth*, 117(B1), 1102. <https://doi.org/10.1029/2011JB008493>
- Yang, H., Liu, Y., & Lin, J. (2012). Effects of subducted seamounts on megathrust earthquake nucleation and rupture propagation. *Geophysical Research Letters*, 39, L24302. <https://doi.org/10.1029/2012GL053892>
- Yang, H., Liu, Y., & Lin, J. (2013). Geometrical effects of a subducted seamount on stopping megathrust ruptures. *Geophysical Research Letters*, 40, 2011–2016.
- Zhang, F., Lin, J., & Zhan, W. (2014). Variations in oceanic plate bending along the Mariana trench. *Earth and Planetary Science Letters*, 401, 206–214. <https://doi.org/10.1016/j.epsl.2014.05.032>
- Zhang, F., Lin, J., Zhou, Z., Yang, H., & Zhan, W. (2018). Intra- and intertrench variations in flexural bending of the Manila, Mariana and global trenches: Implications on plate weakening in controlling trench dynamics. *Geophysical Journal International*, 212, 1429–1449. <https://doi.org/10.1093/gji/ggx488>
- Zhang, J., Sun, Z., Xu, M., Yang, H., Zhang, Y., & Li, F. (2018). Lithospheric 3-D flexural modelling of subducted oceanic plate with variable effective elastic thickness along the Manila Trench. *Geophysical Journal International*, 215, 2071–2092. <https://doi.org/10.1093/gji/ggy393>
- Zhang, J. Y., Xu, M., & Sun, Z. (2020). Lithospheric flexural modelling of the seaward and trenchward of the subducting oceanic plates.

- International Geology Review*, 62(7–8), 908–923. <https://doi.org/10.1080/00206814.2018.1550729>
- Zhang, J. Y., Zhang, F., Lin, J., & Yang, H. (2021). Yield failure of the subducting plate at the Mariana Trench. *Tectonophysics*, 814, 228944. <https://doi.org/10.1016/j.tecto.2021.228944>
- Zhou, Z., & Lin, J. (2018). Elasto-plastic deformation and plate weakening due to normal faulting in the subducting plate along the Mariana Trench. *Tectonophysics*, 734, 59–68. <https://doi.org/10.1016/j.tecto.2018.04.008>
- Zhou, Z., Lin, J., Behn, M. D., & Olive, J. A. (2015). Mechanism for normal faulting in the subducting plate at the Mariana Trench. *Geophysical Research Letters*, 42, 4309–4317. <https://doi.org/10.1002/2015GL063917>
- Zhou, Z., Lin, J., & Zhang, F. (2018). Modeling of normal faulting in the subducting plates of the Tonga, Japan, Izu-Bonin, and Mariana trenches: Implications for near-trench plate weakening. *Acta Oceanologica Sinica*, 11, 53–60.
- Zhu, G., Wiens, D. A., Yang, H., Lin, J., Xu, M., & You, Q. (2021). Upper mantle hydration indicated by decreased shear velocity near the Southern

Mariana Trench from Rayleigh wave tomography. *Geophysical Research Letters*, <https://doi.org/10.1029/2021GL093309>

#### SUPPORTING INFORMATION

Additional supporting information may be found in the online version of the article at the publisher's website.

Supplementary Material

**How to cite this article:** Zhang, J., Zhang, F., Yang, H., Lin, J., & Sun, Z. (2021). The effects of plateau subduction on plate bending, stress and intraplate seismicity. *Terra Nova*, 00, 1–10. <https://doi.org/10.1111/ter.12570>